



# Integrated Electrical Resistivity Tomography and Ground Penetrating Radar Measurements Applied to Tomb Detection

Rita Deiana<sup>1</sup> · Jacopo Bonetto<sup>1</sup> · Alessandro Mazzariol<sup>1</sup>

Received: 15 February 2018 / Accepted: 4 August 2018 / Published online: 19 August 2018  
© Springer Nature B.V. 2018

## Abstract

The integrated use of electrical resistivity tomography (ERT) and ground penetrating radar (GPR) measurements, and in particular the joint analysis of 2D and 3D data, can represent a valid solution for target identification at complex archaeological sites. A good example, in this respect, is given by the case study of a Phoenician–Punic necropolis in the archaeological site of Nora, in southern Sardinia (Italy), where GPR and ERT measurements were collected before site excavation. In this specific case, the mix of soil and air in the buried chambers, as well as the orientation and the complex spatial distribution of these structures into the sandstone bedrock, generated a number of anomalies difficult to interpret only using 2D results. Only the integration of all GPR and ERT data in a 3D view, and the comparison with archaeological evidence after the excavation, allowed a solid interpretation of geophysical anomalies visible in the 2D sections. Overall, this case study demonstrates the efficiency of the combined use of GPR and ERT acquisitions and shows how, in general, only the joint analysis of 2D data and in a 3D view can help the interpretation of the real distribution of the buried archaeological remains at similar archaeological complex sites.

**Keywords** Electrical resistivity tomography · Ground penetrating radar · Tomb detection · Phoenician–Punic necropolis

## 1 Introduction

Archaeological research has shown, over the past two decades, a renewed interest in geophysical prospecting, undoubtedly thanks to the new perspectives offered by the most recent instruments and methods, capable of providing higher resolution and the possibility of acquiring a larger number of data in shorter times, with increased efficiency and greater field productivity (Gaffney and Gater 2003; Linford 2006; Witten 2006; Cardarelli et al. 2008; Ernenwein and Kvamme 2008; Gaffney 2008; Novo et al. 2008; Campana and Piro 2009; Gaffney 2009; Nuzzo et al. 2002; Trinks et al. 2010; Utsi 2010; Batayneh 2011; Fassbinder 2011; Loke et al. 2013). In this respect, two geophysical methods, in recent years, gained more extensive use in the archaeological

---

✉ Rita Deiana  
rita.deiana@unipd.it

<sup>1</sup> Department of Cultural Heritage, University of Padova, Piazza Capitaniato, 7, 35139 Padua, Italy

context: ground penetrating radar (GPR) and electrical resistivity tomography (ERT). The use of these methods in this field, either individually or in combination, is widely documented in the recent literature (Papadopoulos et al. 2006, 2009; Utsi 2010; Berge and Drahor 2011; de Silva et al. 2014; López et al. 2015; Küçükdemirci et al. 2017). In particular, the capabilities of GPR, known for several decades in the archaeological field, have been recently enhanced in terms of surveys' speed, using multichannel systems to cover large investigation areas (Leckebusch 2005; Francese et al. 2009; Trinks et al. 2010, 2018), also in terms of data processing and visualization (Nuzzo et al. 2002; Ernenwein and Kvamme 2008; Goodman et al. 2011, Novo et al. 2012; Conyers 2015a, b; Zhao et al. 2015a, b, 2016; Verdonck et al. 2013, 2015; Economou et al. 2017; Özkan and Samet 2017; Samet et al. 2017). These advances make it possible to identify, quickly and with excellent resolution, the presence of structural remains, placed at shallow depth, provided that the soil does not have high electrical conductivity (Leckebusch et al. 2001; Neubauer et al. 2002; Leckebusch 2003; Berard and Maillol 2008; Booth et al. 2008; Belina et al. 2009). GPR can be considered also the best noninvasive method for archaeological research in an urban context (Leucci 2006; Leucci and Negri 2006; Trinks et al. 2009; Drahor 2011; Strapazon et al. 2013). This is particularly true inside buildings or on paved surfaces where, for example, the use of ERT faces the logistical limitations of placing electrodes in galvanic contact with the ground (Leucci 2006; Athanasiou et al. 2007; Tsokas et al. 2008; Papadopoulos et al. 2009).

On the contrary, in extra urban and rural contexts, the joint use of GPR and ERT is often a winning strategy to tackle the complex, small scale, stratified and laterally varying situation of archaeological sites. For example, it is known that both the GPR and the ERT are excellent methods for the detection of the presence of voids and underground cavities (Piro et al. 2001; El-Qady et al. 2005; Cardarelli et al. 2006; Kofman et al. 2006; Piscitelli et al. 2007; Boubaki et al. 2011; Putiška et al. 2012, Bottari et al. 2017). For this reason, their application also in the archaeological context has found ever wider use (Edwards et al. 2000; El-Behiry 2000; Piro and Goodman 2008; Piro and Gabrielli 2009; Abbas et al. 2012; Ekinici et al. 2012; Testone et al. 2012, 2015; Orlando 2013; Leucci et al. 2016). However, although a cavity represents an ideal target for both GPR and ERT measurements, in terms of contrast of physical properties with the hosting materials, different factors may contribute to making cavity identification and localization an uncertain task using both ERT and GPR. Among these factors, we highlight: (a) the small distance between different cavities (e.g., having a very thin separation wall); (b) the presence of small voids placed at great depths; (c) the presence of voids and cavities, different in size and orientation, totally or partially overlapped; and (d) the presence of cavities partially filled with soil or with soil mixed with waste or stones. In such conditions, the exact identification of each cavity can be problematic, in particular for GPR and ERT measurements taken from the ground surface using only 2D configurations. In fact, as shown in the most recent literature (Negri et al. 2008; Abbas et al. 2012; Orlando 2013; Arato et al. 2015), only a joint use of 2D and 3D (or pseudo 3D) acquisition patterns, supported by an accurate choice of the acquisition parameters and data processing, can greatly improve the capabilities of GPR and ERT to image cavities. In this context, the goal of this paper is to present a challenging case study that demonstrates how the potential pitfalls of ERT and GPR data interpretation can be overcome if a careful use of joint data cross-checking is made and ancillary supporting data (e.g., excavation results) are considered.

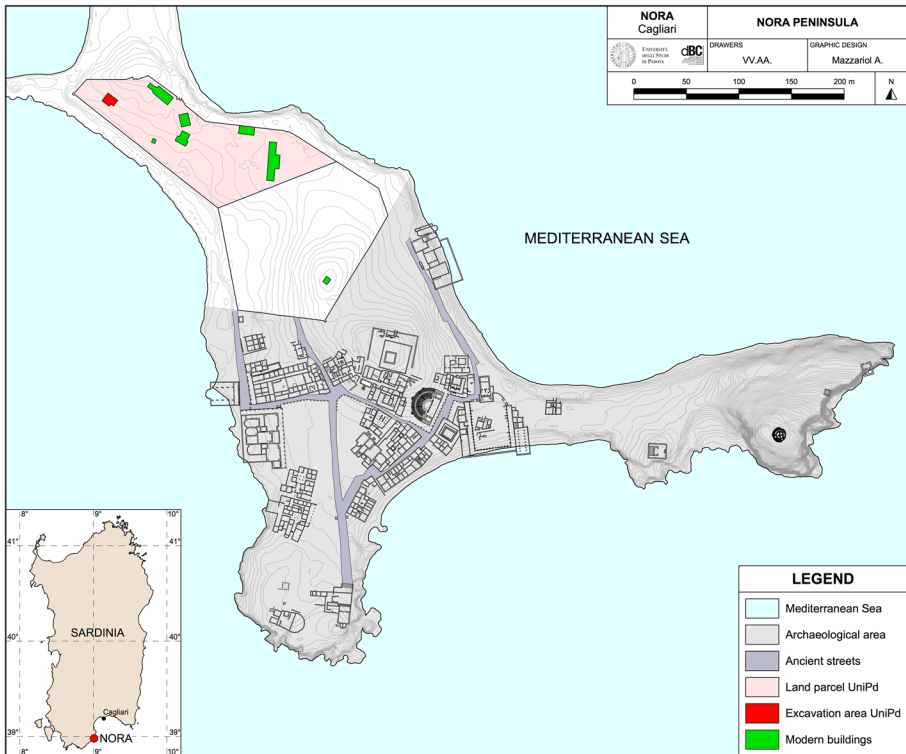


Fig. 1 Map of the studied area of Nora (southern Sardinia-Italy)

## 2 Archaeological and Geological Setting of the Area

The ancient settlement of Nora is located in southern Sardinia, on the promontory of Capo di Pula, which is situated nearly 35 km southwest from Cagliari (Italy) (Fig. 1). The ancient city lies on a narrow peninsula which, due to its morphology, provided an excellent and safe landing-place for the trading ships sailing the Mediterranean Sea in ancient times.

Because of these natural advantages, the area of Nora and its territory, which was directly connected to the region of Sulcis and its metal resources, soon became part and parcel of the sea-routes eastern sailors coming from Greece and from the Near East and established in the West for trading purposes (Botto 2011; Roppa 2013; Bonetto 2014).

The growth of Nora lasted for the whole Hellenistic period, until the city and the whole island of Sardinia were conquered by Rome (238–227 BC), and annexed to its territories as *Provincia Sardiniae et Corsicae* (Bonetto 2009, 2016a). However, Nora’s development and urban plan did not undergo an abrupt change until the second half of the first-century BC, when the urban area was gradually rearranged starting from the construction of the Roman forum, located in the city center to underline the administrative transition of the city which gained the status of *municipium optimo iure* (Bonetto 2002; Bonetto and Ghiotto 2017). From the late fifth-and the sixth-century AD, as a consequence of the disruption of the Roman Empire, the city began a phase of decline during which the roads and the infrastructure networks were gradually abandoned (Bonetto and Ghiotto 2013). The city,

reduced to a landscape of ruins, became a quarry of stone materials which were used to build the earliest dwellings of the medieval village of Pula, which lies a few km inland. The story of the archaeological research at Nora is strictly connected to the discovery of the oldest cemeteries of the settlement (Bonetto 2016b), which are the main focus of this paper.

Other issues to be discussed concern the geological context. The buried chamber investigated until now is dug on the surfaces of the local sedimentary fine-grained and soft sandstone (called “*panchina tirreniana*”) composed by beach conglomerations, arenitic conglomerations, cross-bedding sandstones and unconsolidated sands. This bedrock, easy to cut with metal tools, is characterized by intermediate porosity and permeability which are unable to prevent the infiltration of marine water at sea level depth (Di Gregorio et al. 2000). This has been demonstrated during the recent excavations by the recurrent presence of salt water inside the Punic underground chambers whose depth reached the sea level.

The direction of the natural rock layers is  $45^{\circ}\text{NE}$ , their immersion is toward W, and the inclination is very low. Indeed, the rock surface shows a very modest slope toward southwest. Although the whole surface of the area where the tombs have been unearthed seems to be nearly horizontal, recent excavations made in 2017, after the geophysical investigation, revealed that in ancient times only a small portion of this funerary area was characterized by a flat surface, while other areas were marked by a more articulated soil morphology, with sloping stretches, shallow valleys, and areas located at different heights.

### 3 The Archaeological Researches (2012–2017)

In 2012, the disposal of the military base allowed the Office for archaeological heritage in Cagliari and the Archaeological Mission active in Nora since 1990<sup>1</sup> to conduct research in the central area of the isthmus. Up to now, four archaeological campaigns were conducted, carrying out topographic surveys and stratigraphic excavations, as well as geophysical acquisitions discussed in a specific section of this paper. All these activities contribute in different ways to provide new fundamental information about the funerary areas and the evolution of the settlement during centuries.

In order to organize the field work, the area was first cleaned up from vegetation, as it was entirely covered by dense Mediterranean scrub and small or medium-sized bushes. Later, the area was also cleaned up from plastic and metal waste, in order to reduce the noise in the geophysical data and in general to make field work easier.

First a topographic survey was performed using a Leica TS06 Plus total station, hooked up to some geo-referenced landmarks. The collected data were processed with a CAD software<sup>2</sup> based on Plate Carrée/WGS84 projections. Thanks to this preliminary georeferencing, we created the base map for the geophysical measurements and for the later archaeological excavations, which immediately highlighted very interesting traces related to the early stage of the settlement in this area.

Particular attention was dedicated to the northwestern part of the former military base, where the geophysical survey provided reliable indications about underground anomalies

<sup>1</sup> The Archaeological Mission in Nora is sustained by the Universities of Padova, Milano, Genova and Cagliari. The Soprintendenza Archeologia Belle Arti Paesaggio coordinates the activities with appreciated efforts.

<sup>2</sup> Nemetschek Vectorworks 2013®.



and possible archaeological evidence. Starting from this preliminary information, the excavations carried out from 2012 to 2017 confirmed the presence of a large number of tombs, parts of an undiscovered Phoenician and Punic funerary area of this settlement.

### 3.1 The Phoenician Tombs

The archaeological excavations, carried out in a small part of the larger area previously investigated by means of geophysical measurements, affected about 100 square meters. Ten Phoenician tombs, in general well preserved despite the many historical events, modifications and reuse of this area during the millennia, have been localized here (Fig. 2). These Phoenician tombs consist of small pits dug into the bedrock, in general characterized by a regular layout with unfinished internal surfaces, used for the direct deposition of the burnt human remains with small grave goods or hosting cinerary urns filled with human ashes obtained by the cremation *post mortem*. Some of these very shallow tombs, excavated in the bedrock and differently oriented in the area, have an almost rectangular shape (Fig. 3a), and their size does not exceed 0.7 m×0.35 m, for a depth of 0.55 m (T6, T7 and T11), while most of these have a square shape (Fig. 3b) with a side of 0.35 m and the same depth in the bedrock (T2, T16, T18, T20 and T21). Only in the case of two tombs (T10 and T15), the ashes and the grave goods were directly hosted in the shallow irregular pits (Fig. 3c). A hint about these tombs' location was probably originally given by a small mound of soil or stones. Finally, a singular case in the context of this necropolis is represented by the tomb T18, the oldest among these excavated in this site. This square tomb, in fact, with a side of 0.6 and depth of 0.45 m, was covered by a 0.17-m-thick slab of sandstone and contained human ashes and four different ancient vases, well preserved during the millennia thanks to the compacted soil therein. As discussed before, all these ancient tombs were found at very shallow depth below the actual ground level (about 0.5 m), suggesting that the shallower Phoenician tombs were probably damaged in their upper part already during the Roman period, or at the beginning of the twentieth century, when the whole peninsula was used for the cultivation of wheat (Patroni 1904). The funerary treasure and the cinerary urns hosted in the well-preserved tombs provided fundamental information about the trade that the Phoenician community of Nora established with the populations of mainland Italy. In particular, the production and the circulation in the western Mediterranean of the kind of pottery during the early seventh-century BC allow us to date the realization of these tombs to that specific period (Bonetto and Botto 2017).

These tombs represent, up to now, the most ancient evidence of the presence of the Phoenician settlement at Nora, very close to the chronological horizon of the “Stele di Nora” (Amadasi Guzzo 1990) and older than the earliest trace of the huts or of the religious structures found in the central area of the settlement. These archaeological evidence also reveal that the cemetery area was used for the ritual of cremation by the first Phoenician merchants who established one of their main commercial emporium in Nora. The traces of these emporia also survive in a number of sites close to each other along the entire southern coast of the Sardinia Island, making a real commercial network between the Phoenician and the Nuragic populations distributed in the hinterland.

### 3.2 The Punic hypogea

Approximately in the middle of the fifth-century BC, the area of the Phoenician cemetery was reused for the funerary purposes and here has been excavated some Punic *hypogea*,

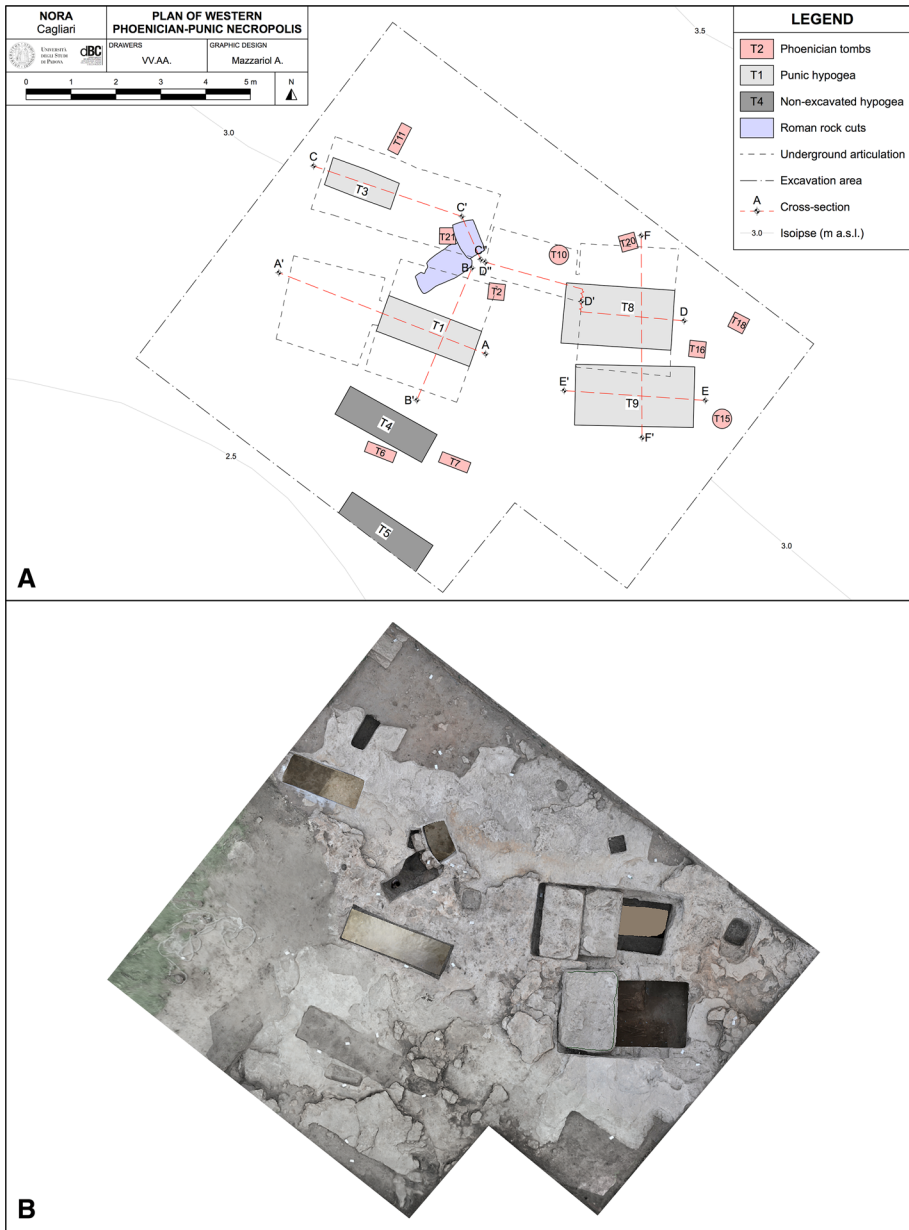


**Fig. 2** **a** Sketch of the western Phoenician–Punic necropolis of Nora (after the 2013–2017 archaeological excavations); **b** top view of the necropolis

where, due to the new burial ritual, the human remains and their grave goods were hosted (Ribichini 2004; Bartoloni 2009, 2015).

In particular, the archaeological excavation carried out from 2014 to 2017 allowed the localization, in the same area, of six different Punic *hypogea*. In this paper, considering



**Fig. 3** Examples of different shapes of Phoenician tombs in the northwestern necropolis of Nora: **a** rectangular (T11); **b** square (T2); **c** irregular pit (T10); see Fig. 2 for the location details

the status of the archaeological field work up to now, we only discuss the evidence provided by four of these *hypogea* (T1, T3, T8 and T9 in Figs. 2, 4, 6, 7), completely emptied, while only two still remain to be excavated (T4 and T5 in Fig. 2). These tombs are composed by rectangular pits with articulated underground chambers (Figs. 4, 6, 7) dug at a significant depth considering the ancient and the actual ground level. In general, the

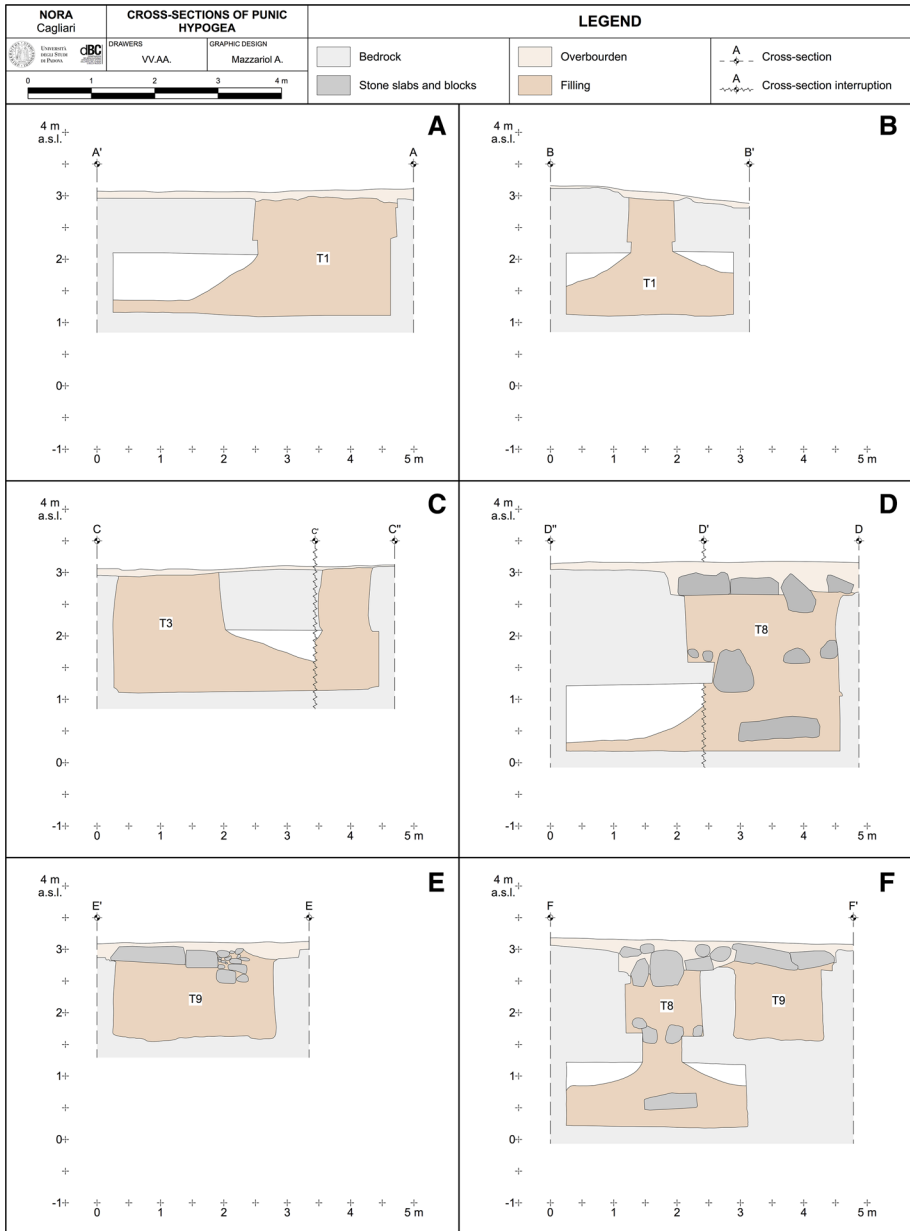


**Fig. 4** Sketch of the sections of Punic tombs in the northwestern necropolis of Nora; for details see Fig. 2

orientation of these *hypogea* is ESE-WNW according to the other Punic necropolis in the eastern bay in Nora (Bonetto et al. 2017b; Mazzariol and Bonetto 2017).

The access to the buried chambers is guaranteed by a rectangular descending well of about 2.1 m × 0.7 m in the tombs T1, T3, T4, T5 (Figs. 2, 4a, b, c, 6b, 7), slightly larger (2.5 m × 1.3 m) in the tombs T8 and T9 (Figs. 2, 4d, e, f, 6a, 7). The archaeological





**Fig. 5** Top view of Punic *hypogea* in the northwestern necropolis of Nora: **a** well access covered with sandstone slabs (T8 and T9 in Fig. 2); **b** well access without sandstone slabs (T1 and T4 in Fig. 2)

excavation also revealed that only the tombs T8 and T9 were still partially covered by broken slabs of sandstone (Figs. 2, 5a), while these slabs have been completely removed from the other four *hypogea* (Figs. 2, 5b). The actual ground level in the area (about 3 m a.s.l.) and the bottom of the deeper buried chamber (about 0.2 m a.s.l.) measured in the tomb T8 (Fig. 4d, d) testify of the ability in the realization of these buried structures excavated and partially overlapped at different depths, in a restricted area. This complex scheme adopted in the necropolis of Nora is undoubtedly different from the one observed in other Punic necropolis (characterized by tombs with *dromos*) in Sardinia, in particular in Sulcis (Bartoloni 1987; Tronchetti 1989) and in Monte Sirai (Bartoloni 2000). Excluding the very simple geometry of the tomb T9 (Figs. 2, 4e, f, 7), in fact, the other tombs present a very complex internal distribution (Figs. 6, 7), probably also due to the further modifications which occurred in the middle of the Roman Imperial Age (approximately in 3rd century AD), when some of these tombs (e.g., T3 in Figs. 4c, 6b, 7) have been transformed into big tanks and partially or totally filled with a mix of sand and silt, pieces of pottery and other waste materials (Bonetto et al. 2017a).

The period of the first use of the underground Punic chambers is suggested by the chronology of the objects found in two unviolated tombs, preliminarily dated between the end of the fifth- and the fourth-century BC. Furthermore, it is important to stress some issues about the spatial extension of the necropolis and its relations with the geomorphological and geological context. Although the interested area appears quite small, other small trenches were excavated recently (2010–2011) and the emerged evidence of rock-cut tombs suggest that this funerary area was not small in size and probably occupied an area of roughly 1 hectare. However, many doubts still existed about the exact position and orientation of the tombs in this larger area; thus, the geophysical surveys appeared absolutely necessary to define the restricted area for the excavations.

About the position of the funerary area within the geomorphological frame, it is quite certain that most of the tombs are located just in the narrowest piece of land between the eastern and western bays, where the maximum distance of the tombs from the shorelines probably does not exceed 30–40 m.



**Fig. 6** Interior of Punic *hypogea* in the northwestern necropolis of Nora: **a** T8; **b** T3; **c** T1; (see Fig. 2 for location details)

#### 4 Geophysical Measurements

In 2013, starting from historical documentation and archaeological evidences gathered a priori, a geophysical survey was conducted on a limited area of  $23.5 \text{ m} \times 7.5 \text{ m}$  ( $176.25 \text{ m}^2$ ) within the larger archaeological site already presented and formerly occupied by the Navy base in the Nora peninsula (Fig. 1). The main goals of the geophysical survey

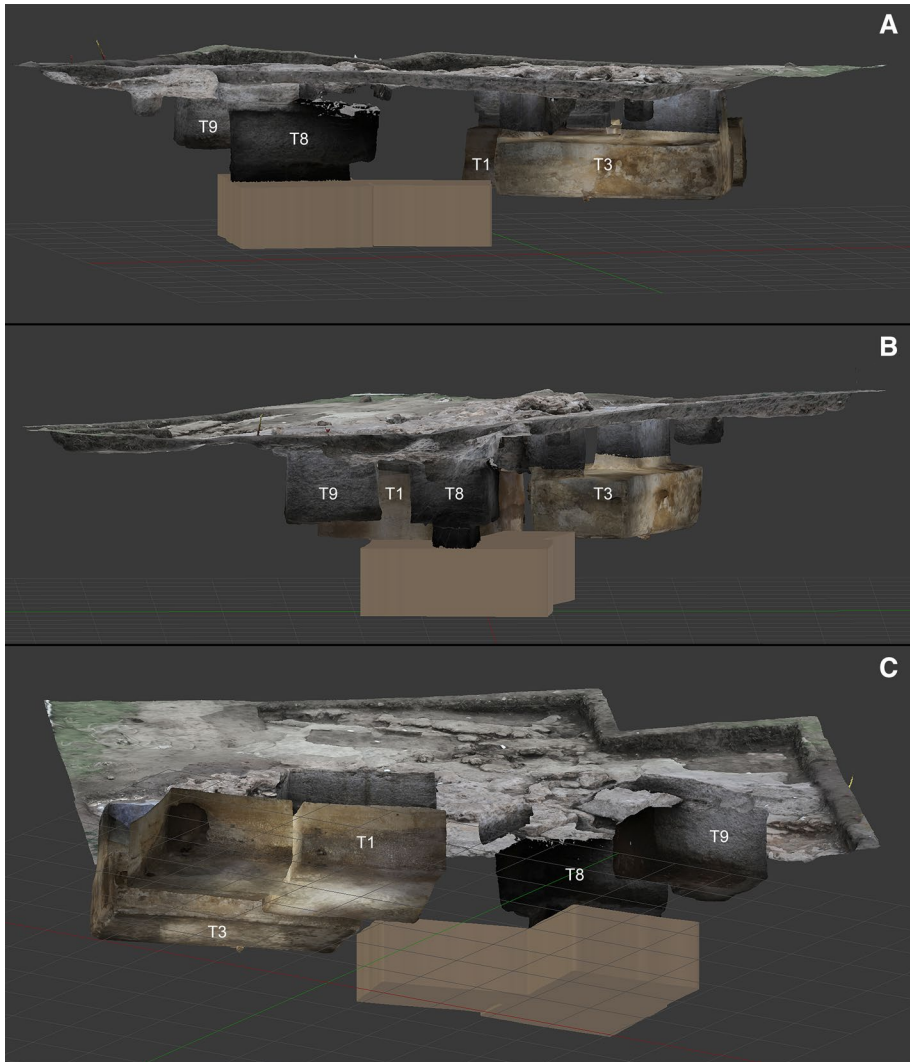


**Fig. 7** 3D view of the necropolis (brown, the 3D view of T8 *hypogeum*'s underground chambers); **a** view from the north; **b** view from the east **c** view from the southwest

in this specific area were to identify the number and the exact location, volume and integrity of undiscovered Phoenician and Punic tombs in the necropolis supposedly hosted here. Starting from the target, the geological setting and the orientation of some tombs excavated in a neighboring area, we decided to collect a number of parallel GPR and ERT lines oriented approximately SE–NW (Fig. 8). Considering the complete abandonment of the former Navy base, before the geophysical surveys, it was necessary to clean the area from vegetation, stones and waste materials (e.g., reinforced concrete and metal waste) scattered on the surface or hidden under the top layer of soil. For this reason, as far as possible, the surface was regularized removing the upper part of the soil (about 5–10 cm). Despite these



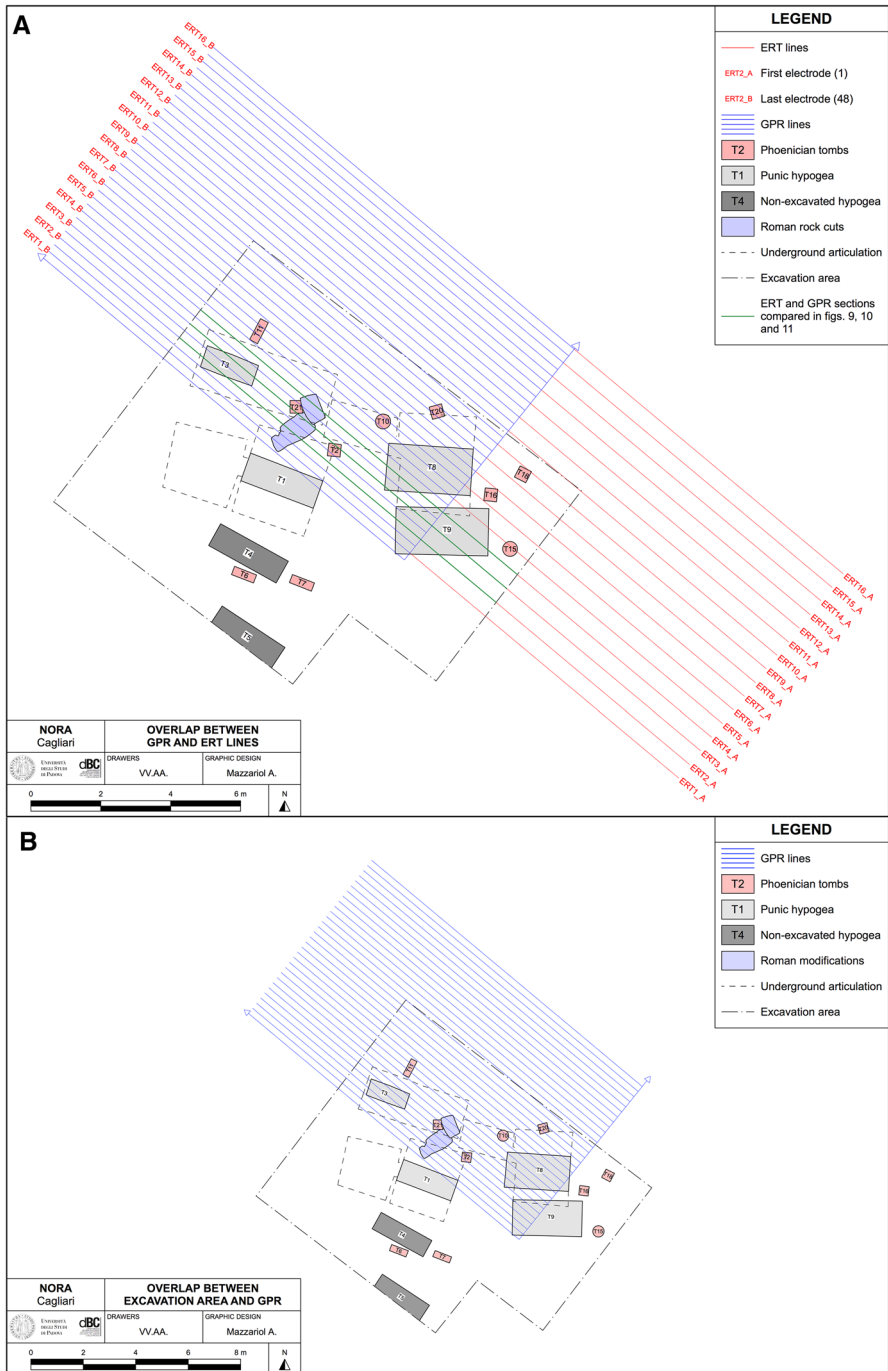


**Fig. 8** Overlapping of GPR and ERT lines and archaeological excavations in the Phoenician–Punic necropolis of Nora

preliminary operations, fundamental to facilitate the GPR acquisitions, the presence in the area of interest of two small trees limited the exact overlapping of the ERT and GPR lines and forced the starting point of the GPR lines 10 m in NW direction, overlapping the ERT lines only for 13.5 m in the same direction.

#### 4.1 Ground Penetrating Radar (GPR)

The GPR measurements were taken using an IDS Ris Hi-Mod Dual frequency system connected to 200–600 MHz monostatic antennas mounted on a cart equipped with a magnetic encoder. The data were collected by moving the monostatic system along parallel transects, using a time window of 64 and 128 ns for the 600 MHz and the 200 MHz antennas, respectively. For both frequencies, we used 512 samples per scan. In all the following interpretation, we assumed a propagation speed equal to 0.1 m/ns. Considering the expected geometry, the complex spatial distribution of the targets and the information gathered a priori we decided to acquire the GPR measurements along parallel transects spaced 0.25 m apart and oriented SE-NW, using the origin of the reference system, as previously described and shown in Fig. 8. This tight acquisition scheme allowed a pseudo 3D reconstruction of the investigated subsoil volume, based on reflection amplitude slices at the different depths of interest and on the building of an isosurface model. All other results (ERT investigations and archaeological excavations) will be related to the same reference system. For GPR data processing, we used ReflexW and GPR-SLICE software for the isosurface model. The processing steps included time zero correction, dewow filtering, vertical signal amplitude recovering and background removal. Although, in general, the data migration allows an improvement in targets identification in the time-slices, in this specific case, without the possibility of having a good estimate of the EM wave velocity in the investigated media (i.e., using a bistatic configuration of antennas) and possible lateral variations of such, we decided not to employ migration processing.

Finally, at the end of the proposed processing steps, the 2D GPR profiles were interpolated using again ReflexW software in order to obtain a pseudo 3D volume and to extract the time-slices at different depths, GPR-SLICE was used to extract the isosurface related to most significant targets in a 3D view. Hereafter, considering the ratio between the maximum depth of interest and the best resolution obtained by two different antennas, we decided to show only the results of the 600 MHz antenna using, as previously described, a constant EM velocity equal to 0.1 m/ns.

#### 4.2 Electrical Resistivity Tomography (ERT)

Based on the early results of the GPR acquisitions, we decided to collect in the same area a series of parallel ERT lines, spaced 0.5 m apart and oriented SE–NW as shown in Fig. 8. The ERT lines overlap 16 GPR lines, over a total length of 13.5 m. This partial overlapping was forced, as previously described, by the presence in the investigated area of two small trees that made the acquisition of the GPR lines cumbersome. The ERT lines were acquired using an IRIS Syscal Pro resistivity meter. For each line, we used 48 electrodes, spaced 0.5 m, for a total length of 23.5 m, using a skip zero dipole–dipole acquisition scheme. For each line, we measured both direct and reciprocal quadrupoles (by swapping potential with current electrodes) in order to estimate the measurement errors (Daily et al. 2004). Each set of data was composed of 2105 measurements, including a complete acquisition of direct and reciprocal resistances

measurements and using an optimized scheme simultaneously using all the 10 physical channels for the voltage of the IRIS Syscal Pro instrument. We set as acquisition parameter a target of 50 mV for the potential readings and a pulse duration of 250 ms for current injection. The repetition error threshold of the resistivity meter measurement cycles was set to 5%, with minimum and maximum number of cycles equal to 3 and 6, respectively. The processing of each of the ERT lines was performed using an Occam inversion approach (LaBrecque et al. 1999) as embedded in the ProfilerR freeware code. The data whose reciprocal error exceeded 5% were excluded as outliers. In general, this criterion implied a loss of approximately 10% of the collected data. The total amount of measurements saved for each line and used for the inversion processing is about 900. Finally, using the inversion results we produced a pseudo 3D distribution of electrical resistivity, obtaining maps at different depths of investigation and a 3D model on the basis of the acquired 2D ERT lines, using the VOXLER3.0 software (Golden Software Inc.).

## 5 Discussion of Geophysical Surveys and Archaeological Excavation Results

In order to discuss the results of the geophysical surveys carried out in the necropolis of Nora, here we will compare them against the evidence emerging from the archaeological excavation in this area. In particular, here we first analyze and compare the results for three GPR and ERT sections, the locations of which are shown in Fig. 8 and which allow us to identify the relative position of these sections with respect to the complex spatial distribution of the burials excavated from 2014 to 2017. The distribution and the extent of the excavated burials (T1, T3, T8 and T9) are shown, respectively, in Figs. 4, 7, and 8. In Fig. 8 the descending wells of the excavated tombs (the total extent of the tombs is represented by dashed lines) are highlighted with dark gray color, where with gray color are indicated the tombs which must be still excavated. These structures are mainly aligned in the ESE-WNW direction, while the ERT and GPR lines run from SE to NW: as a consequence, the GPR and ERT profiles never cross orthogonally the *hypogea*.

In general, the excavation work unearthed a number of structures very close to each other and with buried chambers different in size, also partially overlapped at different depths as in the case of tombs T8 and T9 (Figs. 2, 4f, 7, and 8). Given this excavation evidence, we can compare the images of the excavated volumes against the corresponding 2D GPR and ERT lines collected over some of these structures. To better understand and to clearly represent the spatial complex distribution of these excavated chambers in the bedrock, in particular, Fig. 7 shows a 3D virtual reconstruction. These images are obtained using both Blender and Meshlab software, starting from a 3D photogrammetric relief using SfM (Structure from Motion) technique in the tombs T1, T3, and T9. For the tomb T8, we specify that the SfM relief has not been performed yet. The images reported in Figs. 4, 6, 7, and 8 show how the spatial complexity of the excavated chambers, combined with the different conditions of these burials (violated or non-violated, and thus partially or totally filled with soil), may have influenced the distribution, the size and the consequent interpretation of the anomalies in the geophysical 2D sections.

Considering the origin and the total length of the ERT lines (23.5 m each), we remark that the GPR lines overlap these lines only for a length of 13.5 m, with the GPR lines

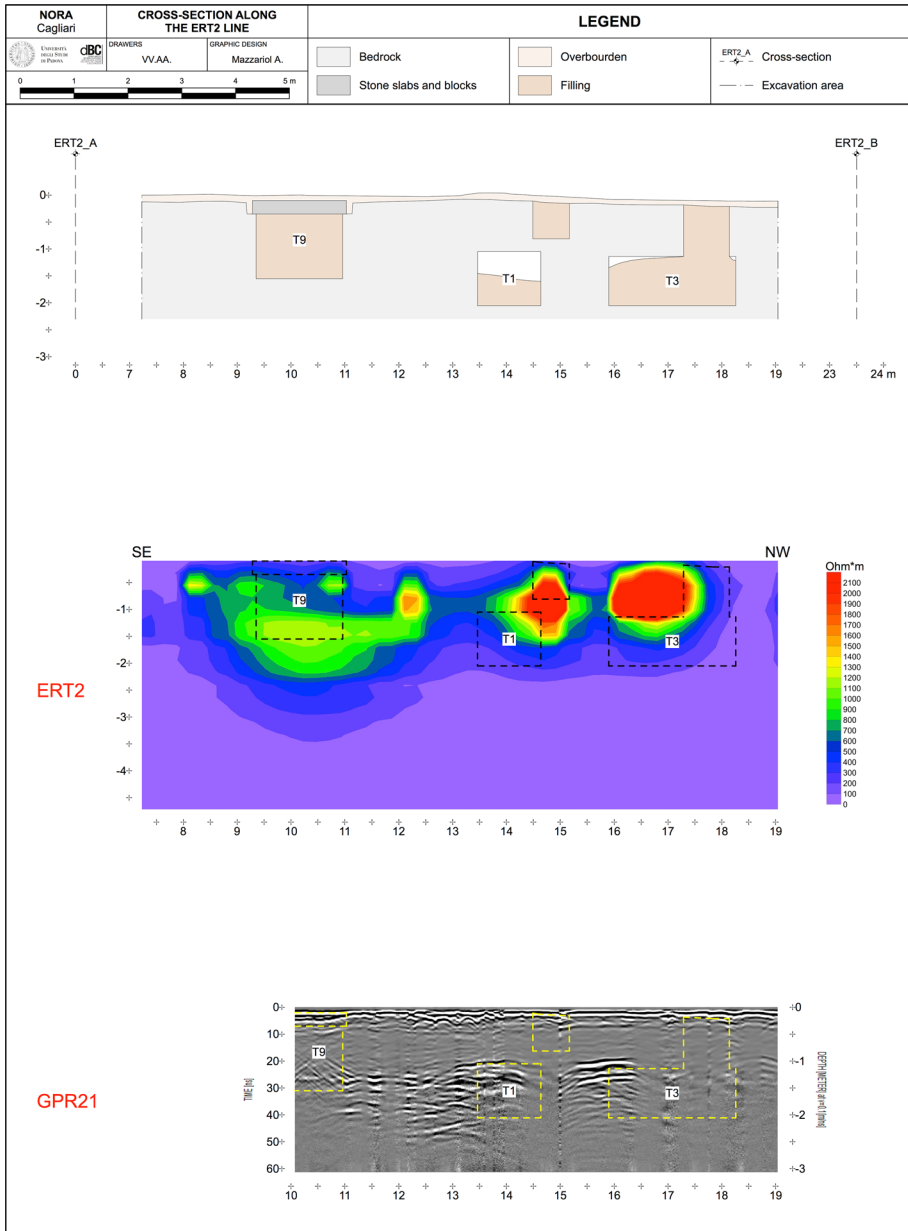


**Fig. 9** Comparison between archaeological and geophysical results (ERT 2 and GPR 21 profiles); see Figs. 8 and 12 for details

starting at 10 m along the ERT lines. We also remark that the excavation work started at 7 m along the ERT line and ended at 19 m along the same line in SE-NW direction (Fig. 8). Note that in the following images (Figs. 9, 10, and 11) the horizontal scale of the geophysical sections (x) always run from SE to NW (from left to right).

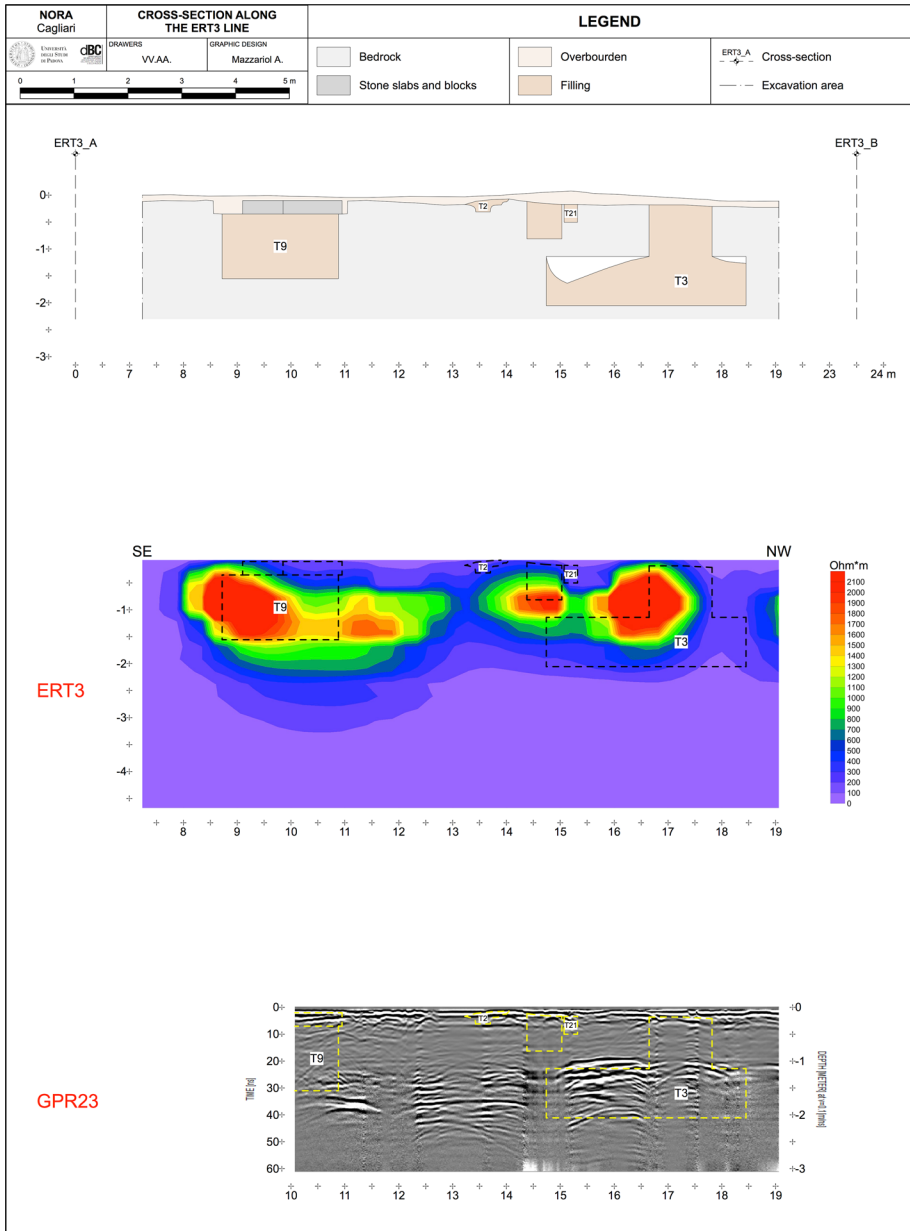


**Fig. 10** Comparison between archaeological and geophysical results (ERT 3 and GPR 23 profiles); see Figs. 8 and 12 for details

Finally, considering the partial overlapping between the different geophysical data and the excavated tombs, the GPR and ERT lines were cut at the edges of the excavation area (see the map in Figs. 8, 9, 10, and 11) for clearer representation.

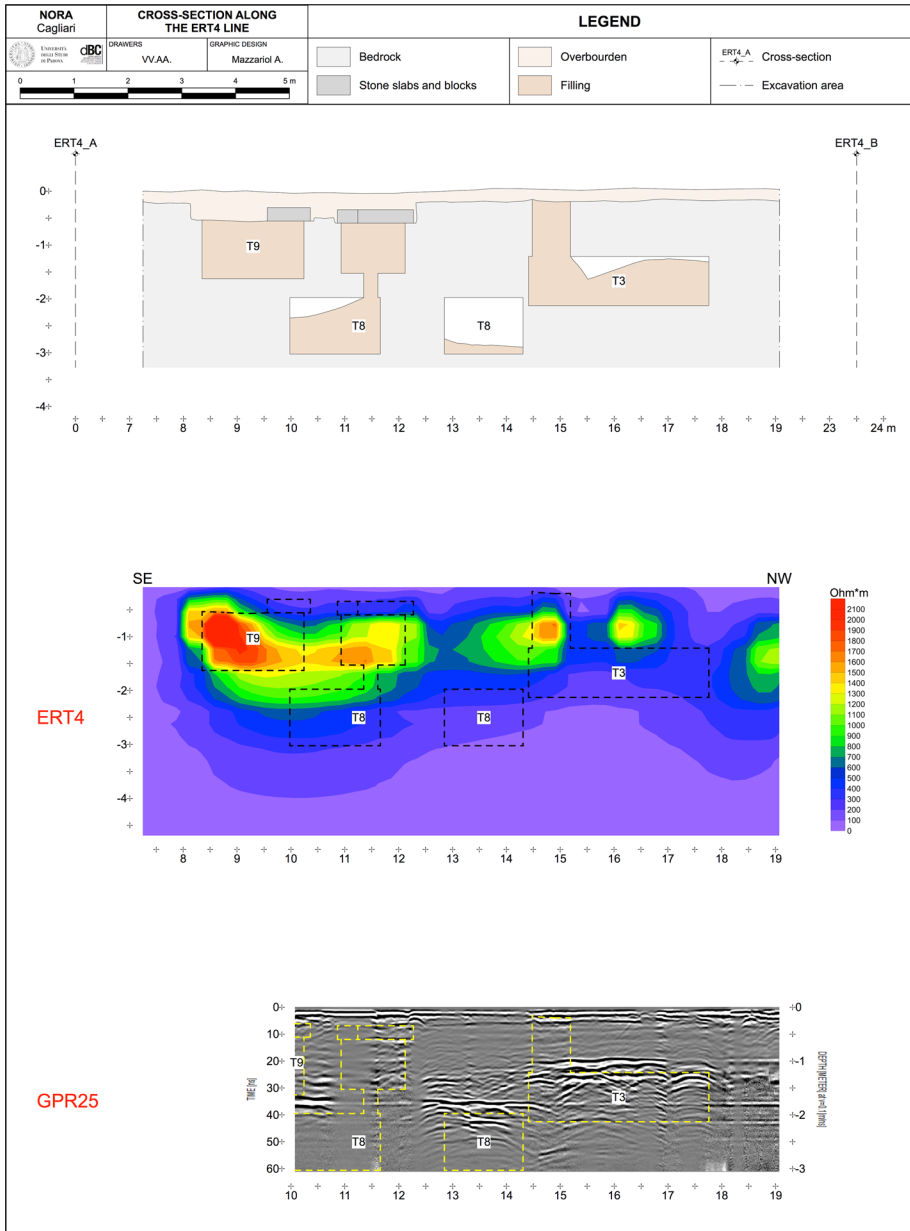


**Fig. 11** Comparison between archaeological and geophysical results (ERT 4 and GPR 25 profiles); see Figs. 8 and 12 for details

Figures 9, 10, and 11 show three ERT and GPR lines: a preliminary analysis of the ERT sections shows the presence of anomalies with high resistivity (red color) normally correlated with the presence of cavities, such as those of interest in this survey, whereas in the GPR sections the maximum amplitude of the reflection of the EM signal and the

reverberation would be associated with the same type of structure. These assumptions are generally true in the case of isolated, empty structures orthogonally crossed by the ERT and GPR lines. However, in this specific case, evidently, the circulation of the electrical and EM signals within these structures with complex and spatially articulated geometries and filled with different materials complicates the a priori interpretation. Figures 9, 10, and 11 show the comparison between geophysical results and actual tomb locations as derived from excavation. The dashed lines shown in the ERT and GPR sections of Figs. 9, 10, and 11, therefore, allow to evaluate the actual correspondence of the anomalies with respect to the excavated structures. Except for the T8 tomb in Fig. 11, all the buried chambers intercepted by these 2D ERT and GPR lines were completely or almost completely filled with soil and waste. Fig. 9, in particular, shows the relative location of ERT line 2, GPR line 21 and the excavated tombs (T9, T1, and T3, going from SE to NW). Considering the locations of the edges of the structures detected by the archaeological excavations, it is clear that the ERT section identifies the structures (e.g., T9) as larger than they actually are.

This is not a total surprise, as ERT inversion is conducted with an Occam approach, that thus seeks the smoothest model that can reproduce the field data within their error level—estimated by reciprocal check. In addition, it is known that any inversion procedure has its own cell dimension which in turn should be fixed according to both vertical and lateral resolution. In this way, the shape of resistivity “anomalies” cannot be expected to match the actual shape/dimension of the buried structures that are sharp contrasts between voids and host rock. Thus, the edges of sharp discontinuities are smeared and the objects appear larger and smoother than they actually are. In addition, the resistivity values are relatively low with respect to expected values for cavities—in fact, as discussed before, most of the cavities are filled or half filled with soil, as a consequence of violation (probably in ancient times). The lower electrical resistivity of the hosting rock, as compared to that expected for the geology of the area, is probably related to the effect of the salt water intrusion visible in some of the excavated chambers.

The GPR data in the same Fig. 9 also require careful considerations to allow a correct interpretation of the anomalies. In particular, the T9 tomb, covered by a sandstone slab (Figs. 4e, f, 5a, 8, 9, 10, and 11), was only partially detected by the GPR acquisition. In this case, the presence of the covering sandstone slab generates a clear effect (i.e., a combination of shallow diffractions) that allows the identification of the lateral boundaries of the structure that is completely filled with soil (i.e., it is a violated tomb). Note also that the GPR signal is clearly attenuated by the relatively high electrical conductivity of the filling material. A very different GPR signal response was collected over tomb T1, as well as over the small subsurface void between tomb T3 and tomb T1, both completely filled with soil. In both cases, a strong GPR signal attenuation, due to the conductive material filling the shallow structures, is apparent. On the other hand, it is interesting to note how GPR data clearly show the presence of a small volume of air inside the partially filled tombs T3 and T1: this causes also strong reverberation of the signal, as apparent in Figs. 9, 10, and 11.

Figure 10 shows a second set of 2D data with ERT line 3 and GPR line 23—again see Fig. 8 for location. These profiles cross over the buried structures T9 and T3. Note also the presence of a shallow pit filled with soil, close to T21, that has a clear effect in terms of GPR attenuation between 14 m and 15 m. GPR also detects the deeper structure of T3, with reverberations in the partially filled void. However, similar to what was discussed for Fig. 9, a number of apparent inconsistencies appear between the geophysical data and the size and the conditions of the excavated structures. This is true both in terms of resistivity values for the ERT sections and in terms of signal attenuation for the GPR data. Both ERT and GPR sections between 11 and 14.5 m detect the presence of possible structures not confirmed up to now, by



the archaeological excavations. In fact, as described before, from 2014 to 2017, only the tombs T1, T3, T8, and T9 were completely excavated and well documented. However, 3D effects, with signals coming from lateral anomalies, shall not be excluded in such a complex environment. Figure 8 confirms the lateral presence of other structures that may explain the anomalies shown in the ERT and GPR profiles.

Figure 11 shows the results of ERT line 4 and GPR line 25 crossing over the T9 and T8 tombs and intercepting these in different positions and at different depths, and finally reaching T3 (see Fig. 8 for reference). Once again, GPR is very sensitive to shallow conductive vs. resistive anomalies in terms of signal attenuation: see the complex effect of the T8 structure on the GPR profile between 10 and 12 m. However, GPR can detect quite well the structures partially filled with soil, e.g., T3 between 14 and 18 m. The ERT section also locates these structures, although not providing precise information on the size and conditions of the tombs (violated or non-violated), as previously discussed.

Overall, it must be noted that the interpretation of the geophysical results is heavily affected by the complexity of the 3D structure of the site (Figs. 7, 8). In fact, the three 2D ERT and GPR sections examined above, as well as the entire dataset acquired in this case study, cross at a slant angle the volumes of the buried structures, having different sizes, and mutual spatial relationships, often being very close to each other, and sometimes overlapping. In addition, the cavities are sometimes (partially or totally) filled with soil. This 3D complexity made particularly challenging the identification of individual structures from the juxtaposition of 2D sections, each of them affected to some extent by lateral 3D effects.

Starting from the evidence which emerged from the archaeological excavation and from the inconsistencies with the anomalies in the ERT and GPR 2D sections, we decided to compare the 2D data with the pseudo 3D view both in a slice map (Fig. 12) and using an isosurfaces view (Fig. 13). In this case, in particular for the slice map (Fig. 12), it is clear that only by superimposing the exact position of the tombs and knowing their real condition (filled or empty) it is possible to evaluate the actual correspondence of the signals with the real distribution of the targets. It should be noted that while in the image of Fig. 12, the GPR and the ERT data provide only a general indication of the area affected by the presence of the tombs (considering the depth of  $-1.3$  m), the images reported in Fig. 13 showing the isosurfaces for ERT and GPR signals allow us (particularly in the case of the GPR) to highlight the presence of different complex structures in the underground, with a good correspondence, for example, with the real geometry of the deeper part of the T8 tomb (see also for comparison the image in Fig. 7). We must take into account that, in most archaeological contexts, the information made available by the historical archives or by any other information source is insufficient to define a priori the exact orientation of expected buried targets, as well as the expected size and geometry. Thus, the problems we face at this site are by no means an exception. In general, we can conclude that only a comparison between 2D and 3D views of the system can help reduce the uncertainties in the interpretation on the real geometry and the spatial distribution of the buried structures. In this sense, the present case study also demonstrates the limits of the pseudo 3D (also called 2.5 D) representation, considering the acquisition geometries and the signal circulation in 2D dimensions, not in a real 3D pattern.

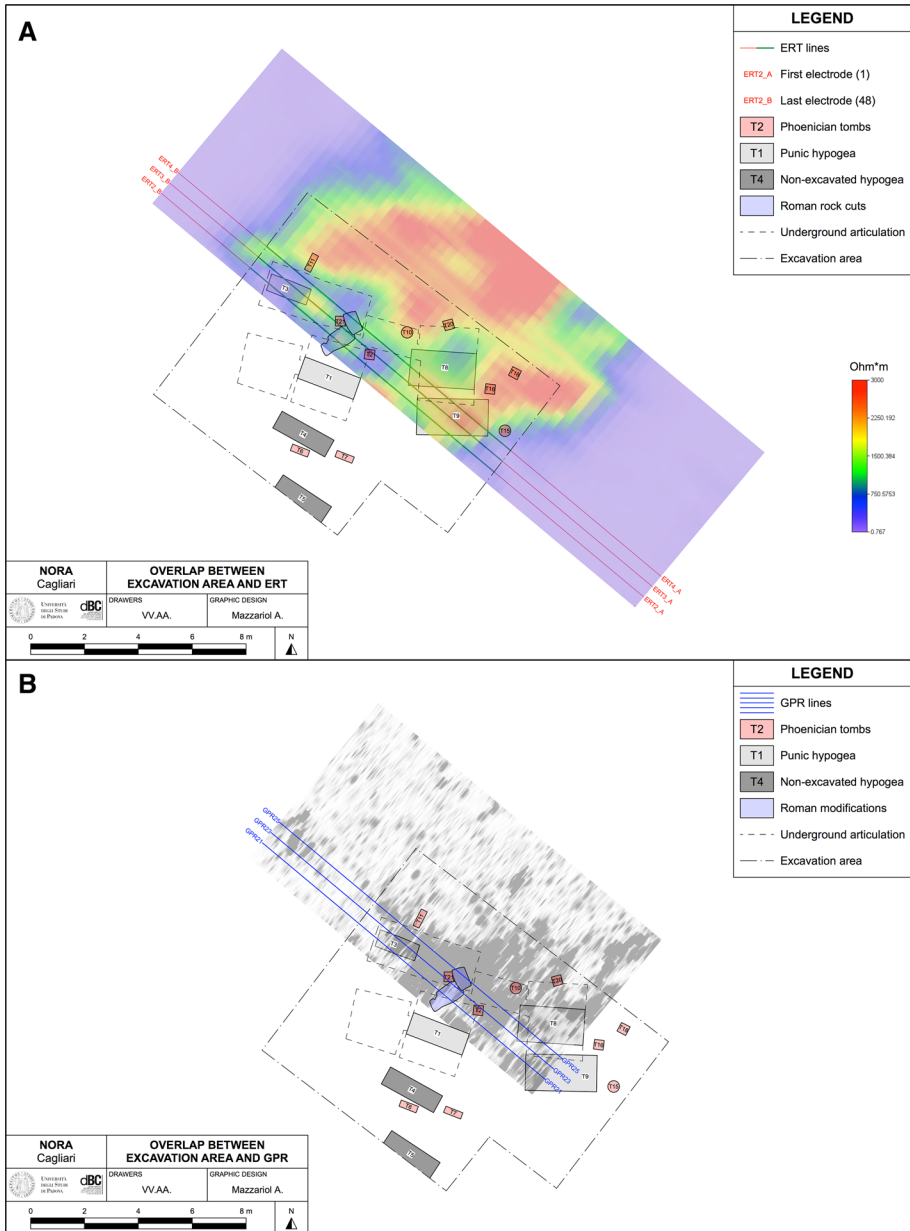
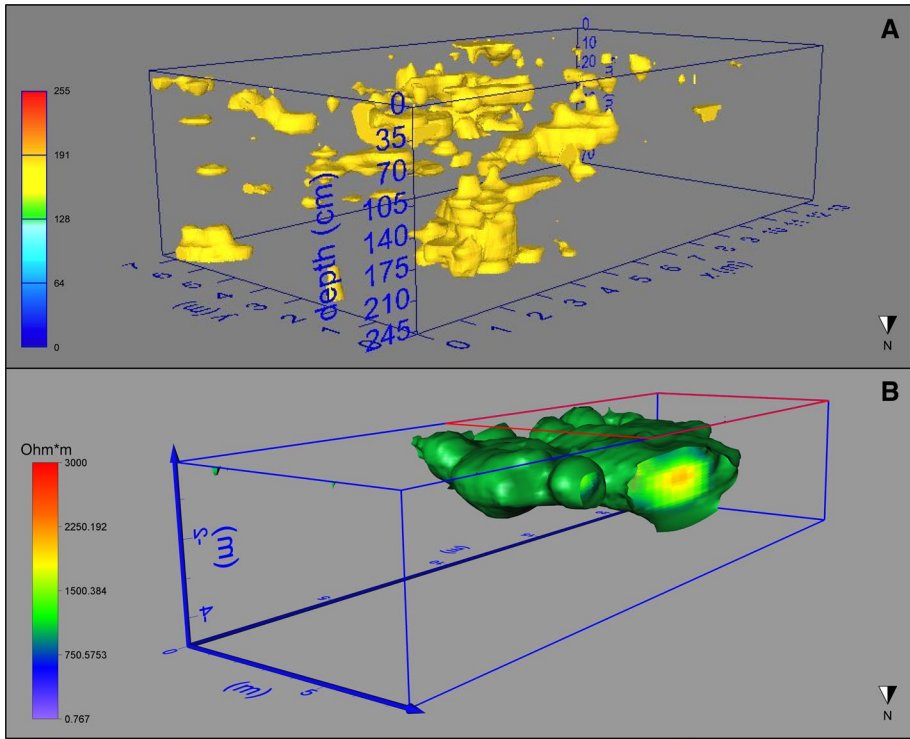


Fig. 12 Slice maps of ERT (a) and GPR (b) at –1.3 m depth overlapped with archaeological evidence

## 6 Conclusions

From the archaeological point of view, the use of geophysical surveys in the site of Nora, despite some problems, has allowed us to detect with high accuracy the presence of some unknown buried tombs, helping their localization before the excavation. Note



**Fig. 13** Comparison between GPR envelope amplitudes (a) and ERT resistivity isosurface (b) obtained by 2D data (see Fig. 8 for more details). The red square in the figure b indicates the position of the GPR data in relation to the ERT measurements

that in most cases the detection of existing archaeological targets is by far more important than the identification of their exact shape. The Punic tombs, made of complex buried volumes accessible through vertical wells, have been often violated and reused over the ages, producing often some modifications in the shape of the original structures and their filling with anthropogenic waste materials and soil. Fortunately, thanks to their complex geometry and their articulation in the deeper part some of these Punic *hypogea* have preserved their integrity. In general, the mix of the Punic buried structures and their modifications with the shallower Phoenician burials certainly create in this necropolis a very complex system.

From a geophysical point of view, this site represents a very challenging case study that helped us to evaluate and discuss the benefits and the limitations of the ERT and GPR surface measurements in complex archaeological sites. Undoubtedly, the presented case of the Phoenician–Punic necropolis of Nora shows a number of different problems that must be taken into account in the acquisition as well as in the interpretation of the data in similar contexts. On the other hand, even though the geophysical data could not resolve entirely the 3D complexity of the site, they still provided key information. The case study demonstrates that only the joint use of 2D ERT and GPR measurements in a pseudo 3D pattern and in particular the comparison of 2D and pseudo 3D results can provide the necessary reliability of the information needed to drive the archaeological excavation.

**Acknowledgements** The authors acknowledge G. Cassiani, G. P. Deidda and G. Vignoli for their support for geophysical acquisitions, G. Leucci for the support for 3D data visualization and also thank for the kind cooperation the Soprintendenza Archeologia Belle Arti e Paesaggio di Cagliari, S. Berto, E. Bridi, F. Carraro, S. Dilaria, L. Zamparo for the archaeological part, G. Martorana and the anonymous reviewers for their helpful comments that greatly improved this manuscript.

**Author Contributions** Jacopo Bonetto contributed to Sects. 2 and 3; Alessandro Mazzariol worked on the description of the Phoenician and Punic tombs in Sects. 3.1 and 3.2 and worked on the graphic details; Rita Deiana developed the geophysical approach and performed the geophysical measurements and the interpretation of the data; all authors contributed to the drafting of the manuscript.

## References

- Abbas AM, Khalil MA, Massoud U, Santos FM, Mesbah HA, Lethy A, Soliman M, Ragab ESA (2012) The implementation of multi-task geophysical survey to locate Cleopatra tomb at tap-Osiris Magna, Borg El-Arab, Alexandria, Egypt “phase II”. *NRIAG-JAG* 1:1–11
- Amadasi Guzzo G (1990) *Le iscrizioni fenicio puniche in Italia*. Istituto poligrafico e Zecca dello Stato, Roma
- Arato A, Piro S, Sambuelli L (2015) 3D inversion of ERT data on an archaeological site using GPR reflection and 3D inverted magnetic data as a priori information. *Near Surf Geophys*. <https://doi.org/10.3997/1873-0604.2015046>
- Athanasiou E, Tsourlos P, Vargemezis G, Papazachos C, Tsokas GN (2007) Non-destructive DC resistivity surveying using flat-base electrodes: near Surface. *Geophysics* 5:263–272
- Bartoloni P (1987) La Tomba 2 AR della necropoli di Sulcis. *Rivista di Studi Fenici XV*, Consiglio nazionale delle ricerche 1:57–73
- Bartoloni P (2000) *La necropoli di Monte Sirai*. I. Collezione di Studi Fenici, 41. Consiglio nazionale delle ricerche, Roma
- Bartoloni P (2009) *Archeologia fenicio-punica in Sardegna*. Introduzione allo studio. CUEC editrice, Cagliari
- Bartoloni P (2015) Il rituale funebre fenicio e punico. In: Mannia S, Buttitta IE (eds) *La morte e i morti nelle società euromediterranee*. Atti del Convegno internazionale Palermo, Palermo, pp 45–58
- Batayneh A (2011) Archaeogeophysics-archaeological prospection—a mini review. *J King Saud Univ Sci* 23:83–89. <https://doi.org/10.1016/j.jksus.2010.06.011>
- Belina FA, Dafflon B, Tronick J, Holliger K (2009) Enhancing the vertical resolution of surface georadar data. *J Appl Geophys* 68:26–35. <https://doi.org/10.1016/j.jappgeo.2008.08.011>
- Berard BA, Maillol JM (2008) Common- and multi-offset ground-penetrating radar study of a Roman villa, Tourega, Portugal. *Archaeol Prospect* 15:32–46. <https://doi.org/10.1002/arp.319>
- Berge M, Drahor M (2011) Electrical resistivity tomography investigations of multilayered archaeological settlements: part II—a case from old Smyrna Höyük. *Prospect, Turkey Archaeol*. <https://doi.org/10.1002/arp.423>
- Bonetto J (2002) Nora municipio romano. In: Khanoussi M (ed) *L’Africa romana*. Lo spazio marittimo del Mediterraneo occidentale. Geografia storica ed economia, Atti del 14. Convegno di studio (Sassari, 7–10 dicembre 2000). Carocci Editore, Roma, pp 1199–1217
- Bonetto J (2009) L’insediamento di età fenicia, punica e romana repubblicana nell’area del foro di Nora. In: Bonetto J, Ghiotto AR, Novello M (ed) *Nora*. Il foro romano. Storia di un’area urbana dall’età fenicia alla tarda antichità, I. Lo scavo, Scavi di Nora 1:41–243. Italggraf editore, Padova
- Bonetto J (2014) L’insediamento fenicio di Nora e le comunità nuragiche: contatti e distanze. In: Van Dommelen P, Roppa A (eds) *Materiali e contesti nell’età del ferro sarda*, Atti della giornata di studi (Museo civico di San Vero Milis, 25 maggio 2012), *Rivista di Studi Fenici* 41:1. Fabrizio Serra editore, Roma, pp 173–182
- Bonetto J (2016a) Nora da colonia cartaginese a municipio romano. In: De Vincenzo S, Blasetti Fantauzzi C (ed.) *Il processo di romanizzazione della provincia Sardinia et Corsica*, Atti del Convegno internazionale (Cuglieri (Or), 26–28 marzo 2015), *Analysis Archaeologica*. An International Journal of Western Mediterranean Archaeology, Monograph series n. 1. Edizioni Quasar, Roma, pp 165–190
- Bonetto J (2016b) Vecchie e nuove conoscenze per lo studio delle necropoli fenicie e puniche di Nora. In: Botto M, Finocchi S, Garbati G, Oggiano I (eds) “Lo mio maestro e ‘l mio autore” Studi in onore di Sandro Filippo Bondi. *Rivista di Studi Fenici*, XLIV, Quasar edizioni, Roma, pp 263–274

- Bonetto J, Botto M (2017) Tra i primi a Nora. Una sepoltura a cremazione nella necropoli sull'istmo. Quaderni della Soprintendenza di Cagliari, 28. Ministero per i Beni e le Attività Culturali, pp 193–214
- Bonetto J, Ghiotto AR (2013) Nora nei secoli dell'Altomedioevo. In: Martorelli R (ed.) Settecento-Millecento. Storia, Archeologia e Arte nei "secoli bui" del Mediterraneo. Dalle fonti scritte, archeologiche ed artistiche alla ricostruzione della vicenda storica. La Sardegna laboratorio di esperienze culturali, Atti del Convegno (Cagliari, 17–19 ottobre 2012). Scuola sarda editrice, Cagliari, pp 271–290
- Bonetto J, Ghiotto AR (2017) Le città della Sardegna in età romana. In: Angiolillo S, Martorelli R, Giuman M, Corda A M, Artizzu D (edd.) La Sardegna romana e altomedievale. Storia e materiali, Corpora delle Antichità della Sardegna. Carlo Delfino editore, Cagliari, pp 45–56
- Bonetto J, Andreatta C, Berto S, Bison L, Bridi E, Covolan M, Dilaria S, Mazzariol A, Ranzato M (2017a) La necropoli fenicio-punica e le infrastrutture romane nell'area della ex Base della Marina Militare. Quaderni Norensi. Padova University Press, 6:169–188
- Bonetto J, Carraro F, Mazzariol A (2017b) Nora e il mare. La necropoli punica orientale: le nuove acquisizioni e il rischio idrogeologico. Quaderni Norensi. Padova University Press, 6:191–199
- Booth AD, Linford NT, Clark RA, Murray T (2008) Three-dimensional, multi-offset ground-penetrating radar imaging of archaeological targets. *Archaeol Prospect* 15:93–112. <https://doi.org/10.1002/arp.327>
- Bottari C, Aringoli D, Carluccio R, Castellano C, D'Ajello Caracciolo F, Gasperini M, Materazzi M, Nicolosi I, Pambianchi G, Pieruccini P, Sepe V, Urbini S, Varazi F (2017) Geomorphological and geophysical investigations for the characterization of the Roman Carsulae site (Tiber basin, Central Italy). *J Appl Geophys*. <https://doi.org/10.1016/j.jappgeo.2017.03.021>
- Botto M (2011) 1992–2002: Dieci anni di prospezioni topografiche a Nora e nel suo territorio. In: Bonetto J, Falezza G (edd.) Vent'anni di scavi a Nora. Formazione, ricerca e politica culturale, Atti della Giornata di studio (Padova, 22 marzo 2010), Scavi di Nora II. Italgraf editore, Padova, pp 59–84
- Boubaki N, Saintenoy A, Tucholka P (2011) GPR profiling and electrical resistivity tomography for buried cavity detection: a test site at the abbaye de l'Ouye (France). In: 2011 6th international workshop on advanced ground penetrating radar (IWAGPR), Aachen <https://doi.org/10.1109/IWAGPR.2011.5963852>
- Campana S, Piro S (2009) Seeing the unseen—geophysics and landscape archaeology. CRC Press, London
- Cardarelli E, Di Filippo G, Tuccinardi E (2006) Electrical resistivity tomography to detect buried cavities in Rome: a case study. *Near Surf Geophys* 4:387–392
- Cardarelli E, Fischanger F, Piro S (2008) Integrated geophysical survey to detect buried structures for archaeological prospecting. A case-history at Sabine Necropolis (Rome, Italy). *Near Surf Geophys* 6:15–20
- Conyers LB (2015a) Ground-penetrating radar data analysis for more complete archaeological interpretations. *Archaeol Pol* 53:202–207
- Conyers LB (2015b) Analysis and interpretation of GPR datasets for integrated archaeological mapping: Multiple GPR datasets for integrated archaeological mapping. *Near surf geophys* 31:2241–2262
- Daily WA, Ramirez A, Binley A, LaBrecque D (2004) Electrical resistivity tomography. *Lead Edge* 23:438–442
- de Silva F, d'Onofrio A, Evangelista L, Fascia F, Silvestri F, Scotto di Santolo A, Sica S, Cavuoto G, Di Fiore V, Punzo M, Vettimo di Scotto P, Tarallo D (2014). Application of ERT and GPR geophysical testing to the geotechnical characterization of historical sites. <https://doi.org/10.13140/2.1.2222.4645>
- Di Gregorio F, Floris C, Matta P (2000) Lineamenti geologici e geomorfologici della penisola di Nora. In: Tronchetti C (ed) Ricerche su Nora, I, anni 1990–1998. Ministero per i Beni e le Attività Culturali, Cagliari, pp 9–17
- Drahor M (2011) A review of integrated geophysical investigations from archaeological and cultural sites under encroaching urbanisation in İzmir, Turkey. *Phys Chem Earth Phys Chem Earth*. <https://doi.org/10.1016/j.pce.2011.03.010>
- Economou N, Benedetto F, Bano M, Tzani A, Nyquist J, Sandmeier KJ, Cassidy N (2017) Editorial of SI: GPR signal processing. *Sig Process*. <https://doi.org/10.1016/j.sigpro.2016.07.032>
- Edwards M, Okita W, Goodman D (2000) Investigation of a subterranean tomb in Miyazaki, Japan. *Archaeol Prospect* 7:215–224
- Ekinci YL, Kaya M, Başaran C, Kasapoğlu H, Demirci A, Durgut C (2012) Geophysical imaging survey in the South Necropolis at the Ancient City of Parion (Kemer-Biga), NW Anatolia, Turkey: preliminary Results. *Mediterr Archaeol Archaeom* 12:145–158
- El-Behiry MG (2000) Nondestructive geophysical surveys for delineating buried tombs and identifying environmental status. In: Proceedings for SAGEEP 2000, Washington D.C., pp 399–406
- El-Qady G, Hafez M, Abdalla MA, Ushijima K (2005) Imaging subsurface cavities using geoelectric tomography and ground-penetrating radar. *J Cave Karst Stud* 67:174–181

- Ernenwein EG, Kvamme KL (2008) Data processing issues in large-area GPR surveys: correcting trace misalignments, edge discontinuities and striping. *Archaeol Prospect* 15:133–149
- Fassbinder J (2011). Geophysical prospection: a powerful non-destructive research method for the detection, mapping and preservation of monuments and sites. In: CEUR workshop proceedings, 806. 1
- Francesca R, Finzi E, Morelli G (2009) 3-D high-resolution multi-channel radar investigation of a Roman village in Northern Italy. *J Appl Geophys* 67:44–51. <https://doi.org/10.1016/j.jappgeo.2008.09.004>
- Gaffney C (2008) Detecting trends in the prediction of the buried past: a review of geophysical techniques in archaeology. *Archaeometry* 50:313–336. <https://doi.org/10.1111/j.1475-4754.2008.00388.x>
- Gaffney C (2009) Geophysical survey in archaeological field evaluation. *Archaeol Prospect* 16:139–140. <https://doi.org/10.1002/arp.346>
- Gaffney C, Gater J (2003) Revealing the buried past: geophysics for archaeologists. The History Press, UK
- Goodman D, Novo A, Morelli G, Piro S, Kutruher D, Henrique L (2011). Advances in GPR Imaging with multi-channel radar systems from engineering to archaeology. In: Proceedings of the symposium on the application of geophysics to engineering and environmental problems, SAGEEP. <https://doi.org/10.4133/1.3614128>
- Kofman L, Ronen A, Frydman S (2006) Detection of model voids by identifying reverberation phenomena in GPR records. *J Appl Geophys* 59:284–299. <https://doi.org/10.1016/j.jappgeo.2005.09.005>
- Küçükdemirci M, Özer E, Piro S, Baydemir N, Zamuner D (2017) An application of integration approaches for archaeo-geophysical data: case study from Aizanoi. *Archaeol Prospect*. <https://doi.org/10.1002/arp.1583>
- LaBrecque DJ, Morelli G, Daily W, Ramirez A, Lundegard P (1999) Occam's inversion of 3D ERT data. In: Spies B (ed) Three-dimensional electromagnetics. SEG, Tulsa, pp 575–590
- Leckebusch J (2003) Ground-penetrating radar: a modern three-dimensional prospection method. *Archaeol Prospect* 10:213–240. <https://doi.org/10.1002/arp.211>
- Leckebusch J (2005) Use of antenna arrays for GPR surveying in archaeology. *Near Surf Geophys*. <https://doi.org/10.3997/1873-0604.2005006>
- Leckebusch J, Peikert R, Hauser M (2001) Advances in 3D visualization of georadar data. Archaeological prospection. In: 4th international conference on archaeological prospection, Vienna, pp 143–144
- Leucci G (2006) Contribution of ground-penetrating radar and electrical resistivity tomography to identify the cavity and fractures under the main church in Botrugno (Lecce, Italy). *J Archaeol Sci* 33:1194–1204
- Leucci G, Negri S (2006) Use of ground penetrating radar to map subsurface archaeological features in an urban area. *J Archaeol Sci* 33:502–512. <https://doi.org/10.1016/j.jas.2005.09.006>
- Leucci G, De Giorgi L, Di Giacomo G, Ditaranto I, Miccoli I, Scardozzi G (2016) 3D GPR survey for the archaeological characterization of the ancient Messapian necropolis in Lecce, South Italy. *J Archaeol Sci Rep* 7:290–302. <https://doi.org/10.1016/j.jasrep.2016.05.027>
- Linford N (2006) The application of geophysical methods to archaeological prospection. *Rep Prog Phys*. <https://doi.org/10.1088/0034-4885/69/7/R04>
- Loke M, Chambers J, Rucker D, Kuras O, Wilkinson P (2013) Recent developments in the direct-current geoelectrical imaging method. *J Appl Geophys* 95:135–156. <https://doi.org/10.1016/j.jappgeo.2013.02.017>
- López J, Rey J, Gutiérrez LM, Novo A, Ortiz Villarejo AJ, Armijo M, Galdóne JM (2015) Electrical resistivity imaging (ERI) and ground-penetrating radar (GPR) survey at the Giribaile site (upper Guadalquivir valley; southern Spain). *J Appl Geophys* 123:218–226. <https://doi.org/10.1016/j.jappgeo.2015.10.013>
- Mazzariol A, Bonetto J (2017) Nuovi dati d'archivio e nuove evidenze archeologiche sulla necropoli punica orientale di Nora (Cagliari). In: Fold&R, 390, Associazione Internazionale di Archeologia Classica, Roma
- Negri S, Leucci G, Mazzone F (2008) High resolution 3D ERT to help GPR data interpretation for researching archaeological items in a geologically complex subsurface. *J Appl Geophys* 65(3–4):111–120
- Neubauer W, Eder-Hinterleitner A, Seren S, Melichar P (2002) Georadar in the Roman civil town Carnuntum, Austria: an approach for archaeological interpretation of GPR data. *Archaeol Prospect* 9:135–156
- Novo A, Grasmueck M, Viggiano DA, Lorenzo H (2008) 3D GPR in archaeology: what can be gained from dense data acquisition and processing? In: Proceedings of the 12th International Conference on Ground Penetrating Radar (GPR 2008), Birmingham, pp 16–19
- Novo A, Lorenzo H, Rial F, Solla M (2012) From pseudo-3D to full-resolution GPR imaging of a complex Roman site. *Near Surf Geophys*. <https://doi.org/10.3997/1873-0604.2011016>
- Nuzzo L, Leucci G, Negri S, Carrozzo MT, Quarta T (2002) Application of 3D visualization techniques in the analysis of GPR data for archaeology. *Ann Geophys* 45(2)
- Orlando L (2013) GPR to constrain ERT data inversion in cavity searching: theoretical and practical applications in archeology. *J Appl Geophys* 89:35–47
- Özkan M, Samet O (2017) 3D visualization approach to GPR data. *Commun Fac Sci Univ Ankara* 59:29–40. <https://doi.org/10.1501/commua1-2-0000000102>
- Papadopoulos N, Tsourlos PI, Tsokas GN, Sarris A (2006) 2D and 3D resistivity imaging in archaeological site investigation. *Archaeol Prospect* 13:163–181. <https://doi.org/10.1002/arp.276>
- Papadopoulos NG, Sarris A, Yi MJ, Kim JH (2009) Urban archaeological investigations using surface 3D ground penetrating radar and electrical resistivity tomography methods. *Explor Geophys* 40:56–68



- Patroni G (1904) Nora. Colonia fenicia in Sardegna. Monumenti Antichi, 14, Reale Accademia dei Lincei, Ulrico Hoepli editore-libraio della Real Casa e della R. Accademia dei Lincei, Milano, cc 109–268
- Piro S, Gabrielli R (2009) Multimethodological approach to investigate chamber tombs in the Sabine Necropolis at Colle del Forno (CNR, Rome, Italy). *Archaeol Prospect* 16:1–14
- Piro S, Goodman D (2008) Integrated GPR data processing for archaeological surveys in urban area. In: The case of Forum (Roma, Italy), 2008, 12th international conference on ground penetrating radar, Birmingham, UK. *Proceedings Extended Abstract Volume*
- Piro S, Tsourlos P, Tsokas GN (2001) Cavity detection employing advanced geophysical techniques: a case study. *Eur J Environ Eng Geophys* 6:3–31
- Piscitelli S, Rizzo E, Cristallo F, Lapenna V, Crocco L, Persico R et al (2007) GPR and microwave tomography for detecting shallow cavities in the historical area of Sassi of Matera (Southern Italy). *Near Surf Geophys* 5:275–285
- Putiška R, Nikolaj M, Dostál I, Kušnirák D (2012) Determination of cavities using electrical resistivity tomography. *Contrib Geophys Geod*. <https://doi.org/10.2478/v10126-012-0018-3>
- Ribichini S (2004) Sui riti funerari fenici e punici. Tra archeologia e storia delle religioni. In: Gonzalez Prats A (ed) *El mundo funerario, Actas del III Seminario internacional sobre temas fenicios* (Guardamar del Segura, 3 a 5 de mayo de 2002). Universitat de València, Alicante, pp 43–76
- Roppa A (2013) Comunità urbane e rurali nella Sardegna punica di età ellenistica. Universitat de València, Valencia
- Samet R, Çelik E, Tural S, Şengönlü E, Özkan M, Damci E (2017) Using interpolation techniques to determine the optimal profile interval in ground-penetrating radar applications. *J Appl Geophys*. <https://doi.org/10.1016/j.jappgeo.2017.04.003>
- Strapazzon G, Deiana R, Brogiolo GP (2013) Extensive geophysical investigation in urban environment. The case of the episcopal center of Padua. In: *Non-destructive approaches to complex archaeological sites in Europe: a round-up*, e-publ. ISBN 978-9-461-97109-8, Ghent, 15-17 January 2013, pp 101–102
- Testone V, Longo V, Algeri G, Bottacchi M, Campo D (2012) Ground penetrating radar and geoelectrical surveys to investigate the santa filitica archaeological complex (Northern Sardinia). *Rend Online Soc Geol Ital* 21:675–677
- Testone V, Longo V, Mameli P, Rovina D (2015). Detection of buried tombs by Electrical Resistivity Tomography and Ground Penetrating Radar
- Trinks I, Karlsson P, Biwall A, Hinterleitner A (2009) Mapping the urban subsoil using ground penetrating radar: challenges and potentials for archaeological prospection. *ArcheoSciences* 33:237–240
- Trinks I, Johansson B, Gustafsson J, Emilsson J, Friborg J, Gustafsson C et al (2010) Efficient, large-scale archaeological prospection using a true three-dimensional ground-penetrating radar array system. *Archaeol Prospect* 17:175–186
- Trinks I, Hinterleitner A, Neubauer W, Nau E, Löcker K, Wallner M, Gabler M, Filzwieser R, Wilding J, Schiel H, Jansa V, Schneidhofer P, Trausmuth T, Sandici V, Ruß D, Flöry S, Kainz J, Kucera M, Vonklich A, Seren S (2018) Large-area high-resolution ground-penetrating radar measurements for archaeological prospection. *Archaeol Prospect*. <https://doi.org/10.1002/arp.1599>
- Tronchetti C (1989) S. Antioco. Sardegna Archeologica, 12, Carlo Delfino editore, Sassari
- Tsokas GN, Tsourlos PI, Vargemesis G, Novack M (2008) Non-destructive electrical resistivity tomography for indoor investigation: the case of Kapnikarea Church in Athens. *Archaeol Prospect* 15:47–61
- Utsi E (2010) The use of ground-penetrating radar to extend the results of archaeological excavation. *Near Surf Geophys* 8:415–422
- Verdonck L, Vermeulen F, Docter R, Meyer C, Knies R (2013) 2D and 3D ground-penetrating radar surveys with a modular system: data processing strategies and results from archaeological field tests. *Near Surf Geophys* 11:239–252. <https://doi.org/10.3997/1873-0604.2013007>
- Verdonck L, Taelman D, Vermeulen F, Docter R (2015) The impact of spatial sampling and migration on the interpretation of complex archaeological ground-penetrating radar data: impact of spatial sampling and migration on interpreting GPR data. *Archaeol Prospect*. <https://doi.org/10.1002/arp.1501>
- Witten AJ (2006) *Handbook of geophysics and archaeology*. Equinox, UK
- Zhao W, Tian G, Forte E, Pipan M, Yimin W, Xuejing L, Zhanjie S, Haiyan L (2015a) Advances in GPR data acquisition and analysis for archaeology. *Geophys J Int* 202(1):62–71
- Zhao W, Forte E, Pipan M (2015b) Improved high-resolution GPR imaging and characterization of prehistoric archaeological features by means of attribute analysis. *J Archaeol Sci* 54:77–85
- Zhao W, Forte E, Pipan M (2016) Texture attribute analysis of GPR data for archaeological prospection. *Pure Appl Geophys*. <https://doi.org/10.1007/s00024-016-1355-3>